Applied Catalysis B: Environmental 89 (2009) 326–334

Contents lists available at ScienceDirect

Applied Catalysis B: Environmental

journal homepage: www.elsevier.com/locate/apcatb

Mechanism of heterogeneous catalytic ozonation of nitrobenzene in aqueous solution with modified ceramic honeycomb

Lei Zhao [a,*], Jun Ma [a,b,**], Zhizhong Sun [c], Huiling Liu [a]

[a] School of Municipal and Environmental Engineering, Harbin Institute of Technology, 202 Haihe Road, Harbin 150090, People's Republic of China
[b] National Engineering Research Center of Urban Water Resources, State Key Laboratory of Urban Water Resources and Environment, Harbin Institute of Technology, Harbin 150090, People's Republic of China
[c] School of Chemistry and Materials Science, Heilongjiang University, Harbin 150080, People's Republic of China

ARTICLE INFO

Article history:
Received 30 May 2008
Received in revised form 10 December 2008
Accepted 12 December 2008
Available online 24 December 2008

Keywords:
Heterogeneous
Catalytic ozonation
Ceramic honeycomb
Nitrobenzene
Degradation
Surface hydroxyl groups
Initiation
Hydroxyl radical (•OH)

ABSTRACT

The degradation efficiencies of nitrobenzene in aqueous solution were investigated by semi-continuous experiments in the processes of ozone alone, ozone/ceramic honeycomb (CH) and ozone/modified ceramic honeycomb (MCH). MCH with 1.0% Mn and 0.5% Cu had more pronounced catalytic ability than CH to accelerate the degradation of nitrobenzene, to increase the utilization efficiency of ozone, to improve the concentrations of hydrogen peroxide (H_2O_2) formation and hydroxyl radical (•OH) initiation, and to enhance the removal efficiency of TOC. The modification process of CH with the metals enhanced the density of surface hydroxyl groups, which determines the initiation of •OH from ozone decomposition and the generation of intermediate species on heterogeneous catalytic surface, yielding the acceleration of the degradation of nitrobenzene in aqueous solution. Possible reaction mechanism of ozone with heterogeneous catalytic surface in aqueous solution was proposed, and the formation mechanism of H_2O_2 and •OH was also discussed according to the combined reactions in heterogeneous and homogeneous catalytic systems.

1. Introduction

Ozone is used for many different purposes such as disinfection, algae control, taste, odour and colour removal, oxidation of inorganic pollutants (iron, manganese), oxidation of organic micro- and macro-pollutants as well as the improvement of coagulation [1]. However, ozonation alone has been shown to achieve a very limited mineralization of organic micro-pollutants in drinking water treatment or removal of refractory COD in industrial effluents. Consequently, various advanced oxidation processes (AOPs, such as O_3/H_2O_2, O_3/UV, UV/H_2O_2, Fenton and UV/Fenton reagents, UV/TiO_2, electron beam, and catalytic ozonation) have been investigated as potential methods for degrading organic compounds [2]. Catalytic ozonation is promising as one of AOPs because of its effective use of ozone and its improved treatment ability of organic compounds through radical reactions [3].

Nitrobenzene is listed as a priority pollutant due to its carcinogenesis and mutagenesis [4,5]. Its commercial uses are reduction to aniline, solvent, synthetic products of benzene [6], metal polishes, shoe-black, perfume, dye intermediates [7,8], plastics, explosives, pharmaceuticals [9], pesticides [10] and a combustible propellant [4]. The production of nitrobenzene in the United States was close to 0.75 billion kg for the year 1995 [4]. Therefore, the remediation of nitrobenzene in aqueous solution is of environmental concern because of its toxicity and the quantity of its production. However, nitrobenzene resists to oxidation by conventional chemical oxidation due to the strong electron-withdrawing property of the nitrogroup. Mineralization of nitrobenzene by micro-organisms is prevented due to the effects of toxic and mutagenic deriving from nitrobenzene and its transformation on biological systems, such as nitrosobenzene, hydroxylaminobenzene and aniline [5,7]. In order to afford the inexpensive and effective processes for the water treatment, various biological treatment processes [11–16], chemical reduction methods and AOPs have been studied for the degradation of nitrobenzene in aqueous solution, such as Fe^0 reduction [4,5], photocatalysis [17–21], photoassisted Fenton oxidation [22] and supercritical oxidation [23].

In recent years, heterogeneous catalytic ozonation has received much attention in water treatment due to its high oxidation potential. Several researches have been reported on the

* Corresponding author. Tel.: +86 451 82291644/86283010; fax: +86 451 82368074.
** Corresponding author at: National Engineering Research Center of Urban Water Resources, State Key Laboratory of Urban Water Resources and Environment, Harbin Institute of Technology, Harbin 150090, People's Republic of China. Tel.: +86 451 86282292/86283010; fax: +86 451 82368074.
E-mail addresses: zhaolei999999@126.com (L. Zhao), majun@hit.edu.cn (J. Ma).

0926-3373/$ – see front matter © 2008 Elsevier B.V. All rights reserved.
doi:10.1016/j.apcatb.2008.12.009

degradation of nitrobenzene in aqueous solution by the heterogeneous catalytic ozonation processes. The experimental results indicate that removal efficiency of nitrobenzene is significantly promoted in the presence of heterogeneous catalysts compared with that of ozone alone, including nano-TiO_2 [24], Mn-loaded granular activated carbon (MnO_x/GAC) [25], ceramic honeycomb (CH) [26], Mn-ceramic honeycomb [27] and synthetic goethite [28]. Moreover, except for MnO_x/GAC catalytic ozonation, it is found that the degradation of nitrobenzene follows the hydroxyl radical ($^{\bullet}OH$) oxidation mechanism in the other systems mentioned above. Moreover, the initiation and formation mechanism of $^{\bullet}OH$ is not introduced clearly in the process of heterogeneous catalytic ozonation.

In order to further increase the catalytic activity of CH [26] and develop a convenient operation of Mn [29,30] or Cu catalyst [31] used in the previous studies, the degradation efficiency of organic micro-pollutant, the utilization efficiency of ozone and the formation of H_2O_2 and $^{\bullet}OH$ were investigated in the processes of ozone alone, ozone/CH and ozone/modified ceramic honeycomb (MCH). Nitrobenzene reacts slowly with molecular ozone ($0.09 \pm 0.02\ M^{-1}\ s^{-1}$), reacts quickly with $^{\bullet}OH$ ($2.2 \times 10^8\ M^{-1}\ s^{-1}$) and it does not adsorb on the CH catalyst surface [26]. Therefore, nitrobenzene, as a special indicator of $^{\bullet}OH$ and a major environmental pollutant, is chosen as a target organic compound due to its toxicity of the central nervous system and its refractory nature to conventional chemical oxidation. The originality of the present study is that, based on the characteristic determination of CH and MCH catalysts, the generation mechanism of H_2O_2 and $^{\bullet}OH$ was also discussed from the aspects of ozone transformation, the interaction of ozone with heterogeneous catalytic surface, and the synergistic effect of homogeneous and heterogeneous reactions, which was different from the previous research dealing with oxidation products and reaction pathway of ceramic honeycomb catalytic ozonation for the degradation of nitrobenzene in aqueous solution [26].

2. Experimental

2.1. Materials and reagents

CH (Shanghai Pengyinaihuo Material Factory, China), shaped to a cylindrical monolithic block with a diameter of 50 mm and a length of 50 mm, was used in the experiment. The cell density of CH was 400 cells/in.^{2} with a wall thickness of 0.4 mm, and the weight of a single block of CH was 34.6–35.4 g.

The model water was prepared by spiking 50 $\mu g\ L^{-1}$ nitrobenzene (Beijing Chemical Factory, China, purified by distillation pre-treatment, 99.80%) in Milli-Q water (Millipore Q Biocel system). Other chemicals used in the experiments were analytical grade reagents. Manganese nitrate (Beijing Chemical Factory, China, 50% (w/w) solution), potassium nitrate (Harbin Chemical Factory, China) and copper nitrate (Tianjin Nankai Chemical Factory, China) were used to modify CH catalyst. A diluted sodium thiosulphate solution was used in the experiments for quenching the reaction. Except for volumetric flasks, the other glassware was muffled overnight at 673 K. The volumetric flasks were washed by soaking them in chromic acid and then rinsing with distilled water.

2.2. Catalyst preparation

CH was washed with distilled water, and dried at 373 K overnight, and then stored in a drying vacuum oven prior to the impregnation. MCH was prepared by wet impregnation of CH with appropriate concentrations of metal ions in an aqueous solution of nitrate salt for the metallic catalyst over a period of 4 h, which were $Mn(NO_3)_2$, $Cu(NO_3)_2$ and KNO_3. The mixed solution of nitrate salt contains 6.0% (w/w) $Mn(NO_3)_2$, 7.5% (w/w) $Cu(NO_3)_2$ and 5.5% (w/w) KNO_3 which were the unique concentrations determined through the optimizing experiments. Impregnated MCH was dried at room temperature for 12 h in air, then at 393 K for 12 h, and calcined at 723 K for 4 h. The procedure was repeated until the wash-coat loading reached the target loading percentage of the total monolith weight.

2.3. Ozonation procedure

The experiments were carried out in a cylindrical ozonation reactor (the inside diameter of 50 mm and the volume of 3 L) made of stainless steel, which was shielded to control reaction temperature constantly at 298 ± 0.1 K by a low thermostatic bath (Model DC-3005A, Ningbo Haishutianheng Apparatus Factory, China) flowing through the surrounding water jacket. Ozone was produced from pure oxygen (Harbin Gas Co. Ltd., China, 99.999%) through an XFZ-5 ozone generator (Qinghua Tongli Co. Ltd., China, max. ozone generation capacity 1.5 mg min^{-1}) at a power setting of 40 W, and was subsequently fed into the ozonation reactor to contact thoroughly with water samples through a porous titanium plate at the bottom of the reactor. The concentration of total applied ozone in this experiment was controlled at 1.0 mg L^{-1} (mg ozone/the sample volume). The solid catalysts were fed into the reactor by taking off its base. Before the experimental operation, the reactor was pre-ozonated for 4 min to satisfy any ozone demand in the ozonation reactor, and then was washed several times with distilled water to exclude any possible side effects. In the ozonation experiment, the model water (3 L) with the nitrobenzene concentration of 50 $\mu g\ L^{-1}$ was pumped into the reactor by a MP-20R magnetic pump (Shanghai Xishan Pump Co. Ltd., China) and then circulated at a rate of 4 L min^{-1}. The reaction time was controlled at 2 min for all the samples. Water samples (each being 50 mL) were taken from the ozonation reactor at various reaction times to analyze the residual concentration of nitrobenzene. The oxidation reaction was quenched by the addition of a small amount of sodium thiosulphate solution. In addition, compared to the scavenger effect of buffer solution (HCO_3^-, CO_3^{2-}, $H_2PO_4^-$, and HPO_4^{2-}), the degradation of trace initial nitrobenzene concentration 50 $\mu g\ L^{-1}$ led to a slight conversion of initial pH which could not affect the experiment, and could be neglected. Therefore, the experiments were carried out at initial pH 6.87 in this study without adding any buffer solution to maintain the pH at a constant value.

2.4. Analytical method

The concentration of ozone in the gas was measured by iodometric titration method [32]. The concentration of residual ozone in aqueous solution was measured by spectrophotometer using the indigo method [33]. The concentration of H_2O_2 formed in the oxidation system was determined by the photometric method [34].

Typically a 50-mL sample containing nitrobenzene was extracted using a total volume of 1 mL benzene (Tianjin Kemiou Research and Development Centre of Chemicals, China, HPLC Grade). Nitrobenzene was analyzed by injecting 1 μL of the extracted headspace sample into GC-14C gas chromatography spectrometer (Shimadzu, Japan), using the high purity nitrogen (99.99%) as the mobile phase at a rate of 34 mL min^{-1}. The conditions of GC-14C gas chromatography were as follows—column temperature: 433 K; injector and detector temperature: 483 K. The pH of aqueous solution was measured by PB-10 pH meter (Sartorious, Germany).

X-ray power diffraction (XRD, Model A-41L-Cu, Input Gokv Zokw Co. Ltd., Japan) was used to analyze the crystal phase of the catalyst. X-ray photoelectron spectroscopy (XPS) were carried out using a PHI 5700 multi-ESCA system with Al Kα radiation ($h\nu$ = 1486.6 eV) and the system base pressure was 6.7×10^{-7} Pa. The specific surface

area and the average pore volume of CH and MCH samples were measured according to the Brunauer–Emmet–Teller (BET) method with the krypton adsorption at liquid nitrogen temperature on a Micromeritics ASAP 2020 accelerated surface area and porosity system. Pore volume and pore size were determined by the BJH method. To measure the BET specific surface area of the catalyst monoliths, a particular home-made test tube was needed to host the sample. The density of surface hydroxyl groups was measured according to a saturated deprotonation method described by Laiti et al. [35,36]. The pH at the point of zero charge (pH_{PZC}) was measured with a mass titration method [37,38]. Inductive coupled plasma emission spectrometer (ICP, optima 5300DV, PerkinElmer, USA) was used to determine the concentration of metal ion in aqueous solution.

Electron paramagnetic resonance (EPR) experiment was conducted for the determination of •OH generated in the ozonation process. A nitron spin-trapping reagent of 5,5-dimethyl-1-pyrolin-N-oxide (DMPO), which was purchased from Fluka, was used in the process. In succession, the EPR spectrum was measured at room temperature with an EPR spectrometer (Bruker EMX-8/2.7 ESR 8 spectrometer with ER 4102ST cavity) under the following experimental conditions: X-field sweep; center field 3480.00 G; sweep width 100.00 G; static field 3480.00 G; frequency 9.751000 GHz; power 4.00 mW. The sample was scanned and accumulated 10 times for 20.972×10 s.

Mineralization of pollutant was monitored for total organic carbon (TOC) removal, which was determined with a TOC analyser (Analytic Jena Multi N/C 3100, the realistic measuring limit: 0.015 mg L^{-1}, the accuracy: $\leq \pm 3\%$).

A gas chromatographic and mass spectrometric analysis system (GC/MS, 6890GC/5973MS, Agilent, USA) with 30 m × 0.25 μm × 0.25 mm DB-5 column was used to identify the degradation products. The chromatographic conditions were the following: the initial column temperature was held for 2 min at 333 K, ramped at 5 K min^{-1} to 473 K, and then ramped at 20 K min^{-1} to 553 K. Ultrapure helium was used as the carrier gas at a velocity of 1.0 mL min^{-1}. Before being subjected to GC/MS analysis, the samples were enriched by means of solid-phase extraction (SPE) with HPD-100/300/600 absorbent resins (Cangzhou Chemical Co. Ltd., China) after ozonation. The enrichment column was eluted by ether. Elution rate was 2 mL min^{-1}, and then dehydrated by anhydrous sodium sulphate for 5 min. The filtrate was then concentrated to 1 mL using a K-D concentrator. A splitless injector was used with a column head pressure of 69 kPa, and extract of 2 μL was subjected to GC/MS determination.

Ion chromatography (IC, CDD-6A, Shimadzu Co., Japan) was used to identify organic acid (eluent: 2.5 mmol L^{-1} tris-hydroxymethyl-aminomethane, 2.5 mmol L^{-1} phthalic acid) and inorganic nitrogen species (eluent: 8.0 mmol L^{-1} *p*-hydroxybenzoic acid, 3.2 mmol L^{-1} 1,3-bis[tris(hydroxymethyl)methylamino]propane, 50 mmol L^{-1} boric acid).

3. Results and discussion

3.1. Degradation efficiency of nitrobenzene in the selected processes

The experiments were performed in the selected processes in order to investigate the degradation efficiency of nitrobenzene, including ozone alone, ozone/CH, ozone/MCH, adsorption on CH and adsorption on MCH. The results are shown in Fig. 1.

As represented in Fig. 1, at different reaction times after the treatment of a nitrobenzene aqueous solution of 50 μg L^{-1}, the degradation efficiency of nitrobenzene is higher in the presence of CH catalyst compared to the case when catalyst was absent, and a remarkable oxidation rate is observed for combined ozone and MCH system. Comparing the curves in Fig. 1, it is interesting to emphasize that after 10 min of reaction time, the degradation efficiency of nitrobenzene in the system of ozone alone is 37%, and adsorption on CH and MCH only results in the degradation of 2% and 1%, respectively. Comparing the curve C (ozone/CH) with the cumulative effect of ozone alone and adsorption on CH (the curves A and B), an increment of approximately 19% of nitrobenzene degradation is observed. Under the same experimental conditions, ozone/MCH system leads to about 83% nitrobenzene conversion, indicating an increment of 44% compared to the cumulative effect of ozone alone and adsorption on MCH. From these data, it is deduced the following: (1) nitrobenzene adsorbs slightly on the surface of CH and MCH catalyst, and the modification of CH with the metals can decrease the adsorption of nitrobenzene on the catalyst surface; (2) the presence of CH or MCH catalyst has the synergistic effect with ozone for the degradation of nitrobenzene; (3) the process of modification can improve the catalytic activity of CH.

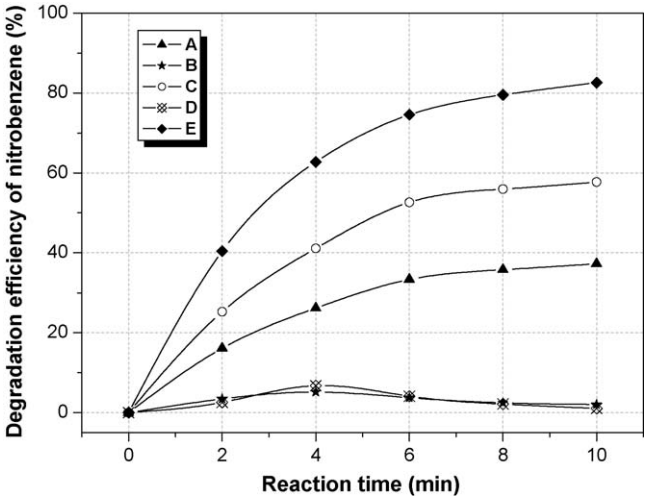

Fig. 1. Comparison of the degradation efficiency of nitrobenzene in the selected processes (reaction conditions—temperature: 298 K; initial pH: 6.87; initial nitrobenzene concentration: 50 μg L^{-1}; the concentration of total applied ozone: 1.0 mg L^{-1}; the amount of CH and MCH catalysts used in series: 58.3 g L^{-1}; (A) ozone alone; (B) adsorption on CH; (C) ozone/CH; (D) adsorption on MCH; (E) ozone/MCH; MCH: modification of CH with 1.0% (w/w) Mn and 0.5% (w/w) Cu).

As we know, heterogeneous catalytic ozonation is a potential alternative AOP. One of the reasons is that the presence of heterogeneous surface appears to transfer ozone into aqueous solution more efficiently [39]. Therefore, it is very significant to investigate the aspect of ozone transfer from gaseous phase to liquid phase.

3.2. The utilization efficiency of ozone in the selected processes

Due to the importance of ozone transfer steps on the heterogeneous catalytic process, the experiments were arranged to investigate the evolution of ozone mass transfer. The mass balance of ozone in gas and liquid phase may be described using the following expression:

$$[O_3]_T = [O_3]_O + [O_3]_R + [O_3]_C \quad (1)$$

where $[O_3]_T$ is the concentration of total applied ozone; $[O_3]_O$ is the concentration of offgas ozone; $[O_3]_R$ is the concentration of residual ozone and $[O_3]_C$ is the concentration of consumed ozone. As a matter of convenience to evaluate, the dimension of Eq. (1) is transferred from mg to mg L^{-1} uniformly. At first, the variation of $[O_3]_O$ was practically identified in the different processes within reaction time of 10 min. The results are represented in Fig. 2.

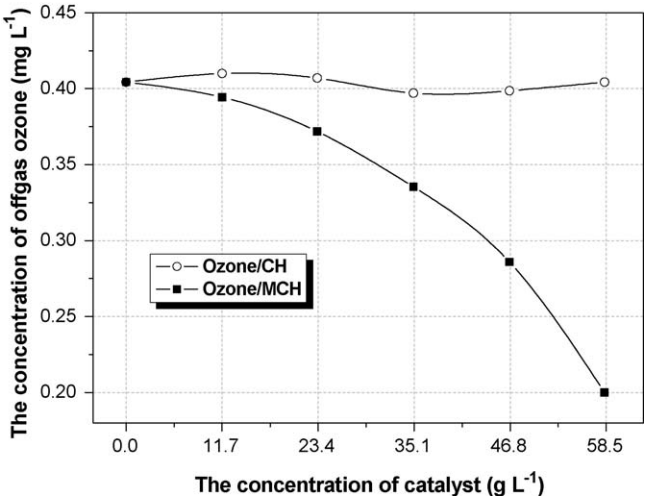

Fig. 2. Relationship of the concentration of offgas ozone and the amount of catalyst in the selected processes (reaction conditions as in Fig. 1).

Fig. 2 depicts the results of the experiments carried out in the presence or absence of CH or MCH catalyst. It can be found that $[O_3]_O$ decreases observably in the presence of MCH. The results also indicate the expected trend, that was, the more the amount of MCH used, the lower the $[O_3]_O$ obtained, which declines smoothly from about 0.40 to 0.20 mg L^{-1} with the amount of MCH catalyst used in series from 0 to 58.3 g L^{-1}. Contrarily, the conversion of $[O_3]_O$ in the ozone/CH process is slight, fluctuating between 0.41 and 0.40 mg L^{-1}. The situation shows that CH catalyst has a stronger resistance to control the stability of $[O_3]_O$.

Another factor affecting the ozone mass transfer in Eq. (1) is $[O_3]_R$. The effects of ozone coupled with catalyst on $[O_3]_R$ in aqueous solution were investigated at several differential initial amounts of CH and MCH, at a fixed total applied ozone of 1.0 mg L^{-1}. These results, which are summarized in Fig. 3, show that $[O_3]_R$ reaches the maximum of 0.43 mg L^{-1} in the process of ozone alone at 4 min, and then decreases to 0.28 mg L^{-1} at 10 min reaction time. However, $[O_3]_R$ in the ozone/CH and ozone/MCH systems present the maximum value at about 3 min and 2 min, respectively. After that time point, $[O_3]_R$ in both the processes decline steadily with the increasing reaction time. Fig. 3 also shows that the more the amount of the catalyst, the less the $[O_3]_R$ in aqueous solution at the end of the treatment. This phenomenon indicates that the introduction of heterogeneous catalyst can accelerate the decomposition and the transformation of ozone, leading to the decrease in concentration of ozone accumulation in aqueous solution.

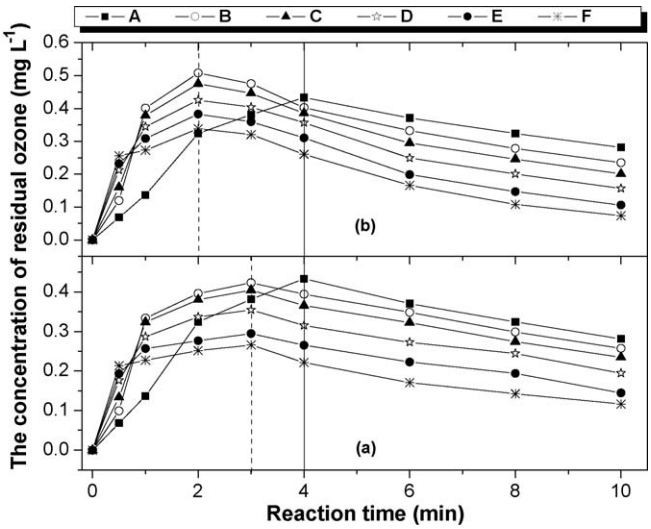

Fig. 3. Evolution of the concentration of residual ozone in the selected processes (reaction conditions as in Fig. 1—(a) ozone/CH; (b) ozone/MCH; (A) ozone alone (without catalyst); (B) catalyst concentration: 11.7 g L^{-1}; (C) catalyst concentration: 23.3 g L^{-1}; (D) catalyst concentration: 35.0 g L^{-1}; (E) catalyst concentration: 46.7 g L^{-1}; (F) catalyst concentration: 58.3 g L^{-1}).

Based on the data of Figs. 2 and 3, $[O_3]_C$ can be calculated from Eq. (1). Therefore, R_U, the utilization efficiency of ozone, can be expressed as follows:

$$R_U = \frac{[O_3]_C}{[O_3]_T} \quad (2)$$

According to the results obtained and Eq. (2), the evolution of R_U with amount of catalyst corresponding to the experiment studied is given in Fig. 4.

Fig. 4 presents the influence of amount of catalyst on R_U in the processes of ozone/CH and ozone/MCH. As can be observed, the increase in amount of catalyst exerts the same influencing rules on R_U in both the catalytic processes, leading to an increase in R_U when amount of CH or MCH catalyst increases from 0 to 58.3 g L^{-1}. From Fig. 4 it also can be observed that, with the same amount of catalyst, ozone/MCH can obtain a higher R_U compared to the case of ozone/CH. According to this phenomenon, it can be deduced that MCH has the higher catalytic activity to improve R_U in the ozonation system. The results, the decrease in $[O_3]_R$ and the increase in R_U, may suggest that the presence of heterogeneous surfaces also helps to initiate the formation of new species from ozone decomposition [33], for example, H_2O_2 and •OH.

3.3. The concentration of H_2O_2 formation in the selected processes

In order to confirm the new species generated from ozone decomposition, the concentration of H_2O_2 formation in the selected processes was investigated. The experimental conditions were similar to those in the previous studies. The results are shown in Fig. 5.

From the data of Fig. 5, it can be found that, as described in the previous study dealing with ozone [40–42], certain concentrations of H_2O_2 are formed as a result of ozone decomposition in the processes of ozone alone, ozone/CH and ozone/MCH at temperature 298 K and initial pH 6.87. The concentration of H_2O_2 formation in the process of ozone/MCH increases continuously to 0.0685 mg L^{-1} with the increasing reaction time to 10 min. However, in the ozone

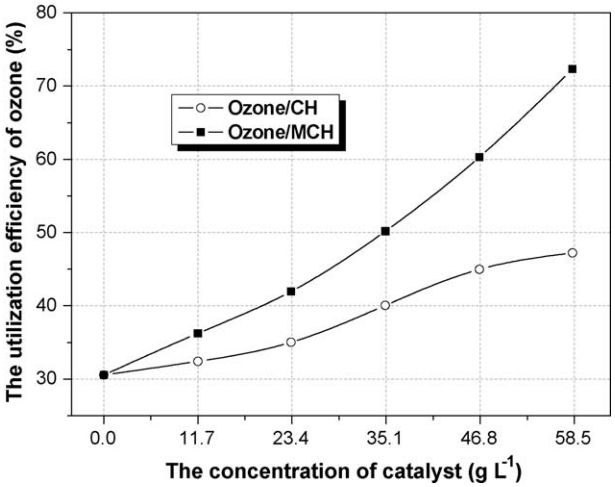

Fig. 4. Relationship of the utilization efficiency of ozone and the amount of catalyst in the selected processes (reaction conditions as in Fig. 1).

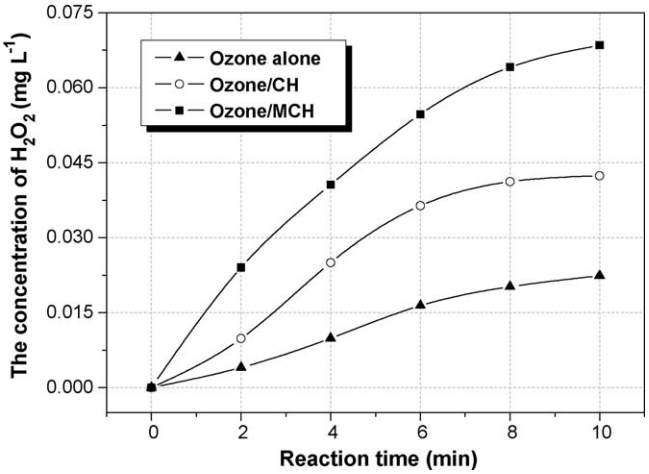

Fig. 5. Comparison of the concentration of H_2O_2 formation in the selected processes (reaction conditions as in Fig. 1).

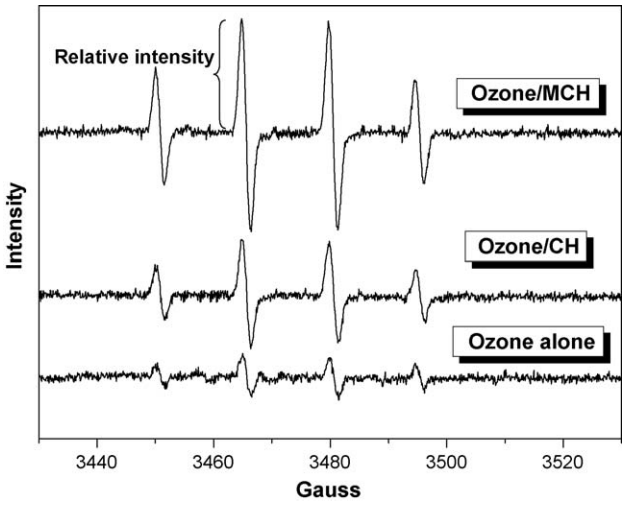

Fig. 6. Comparison of the intensity of DMPO–OH adduct signals in the selected processes (reaction conditions as in Fig. 1; initial DMPO concentration: 100 mmol L^{-1}).

alone and ozone/CH systems, H_2O_2 forms with a rapid rate within the initial 6 min, and then the formation of H_2O_2 slows down until the concentration of H_2O_2 eventually reaches a plateau of 0.0224 and 0.0424 mg L^{-1} at about reaction time 10 min, respectively. Fig. 5 also shows that, in the case of adding CH catalyst, the formation of H_2O_2 is more obvious compared to the case of ozonation alone. Furthermore, the formation of H_2O_2 becomes more pronounced in the presence of MCH catalyst.

In addition, it should be noticed that the results of Fig. 5 only represent the equilibriums concentrations of H_2O_2 because of the series complex matrix reactions in the three selected processes. The concentration of H_2O_2 formation in the reaction solution is too little to have any important accelerating contribution on the degradation efficiency of nitrobenzene. However, as an intermediate species production, it may influence the initiation of other highly oxidative species, such as •OH.

3.4. The detection of •OH formation by EPR in the selected processes

Another significant new species generated from ozone decomposition is •OH. Therefore, it is very important to identify directly whether •OH is generated in the processes of ozonation alone and catalytic ozonation. However, it is very difficult to hold and then measure •OH like other stable substances because it is a kind of short-lived species. EPR enables the detection of radicals, and the spin-trapping/EPR technique has been developed to detect unstable radicals [43]. Unstable free radicals are converted to the corresponding stable spin-adducts by binding spin-trapping reagents, and the spin-adducts are measured by EPR spectroscopy. The pattern of the resulting EPR spectrum is strongly changed by the free radicals bound, and then the type as well as the amount of free radicals can be determined from the EPR parameter and its signal intensity. This technique has been applied to the investigation of •OH generated in AOPs for water treatment [44,45]. For further confirming the reaction mechanism, spin-trapping/EPR technique was also applied for measuring the •OH generated in ozonation alone and catalytic ozonation of the present experiment. Comparison of the intensity of DMPO–OH adduct signals in the selected processes is shown in Fig. 6.

From Fig. 6, it is seen that the typical EPR spectrum appears in the processes of ozone alone, ozone/CH and ozone/MCH at the initial DMPO concentration of 100 mmol L^{-1}. The spectrum is composed of quartet lines having a peak height ratio of 1:2:2:1 and the parameters are hyperfine constants α_N = 1.49 mT, α_H = 1.49 mT and g-value = 2.0055. These parameters coincide with those of the DMPO–OH adduct as demonstrated previously [44]. The experimental phenomenon indicates that the initiation of •OH exists in the three reaction systems mentioned above. It also can be found that the DMPO–OH adduct signals observed in the processes of ozone/CH and ozone/MCH are stronger than the case of ozonation alone. Like H_2O_2 formation, the results of Fig. 6 also suggest that the processes of ozone/CH and ozone/MCH can generate the higher concentration of •OH under the same experimental conditions compared to that obtained from the ozone alone system due to the introduction of heterogeneous surface.

The generation of •OH is the most important characteristic of AOPs. A common objective of heterogeneous catalytic ozonation is to produce •OH in sufficient quantity to improve the mineralization of organic compounds for the micro-pollutants removal in drinking water treatment.

3.5. Removal efficiency of TOC in the selected processes

To investigate the mineralization of organic compounds in the selected processes, the experiments were performed to detect the removal efficiency of TOC in the processes of ozone alone, ozone/CH and ozone/MCH. The results are represented in Fig. 7.

Fig. 7 indicates that the two catalytic ozonation processes are more effective than ozonation alone to remove TOC from aqueous solution containing nitrobenzene. 41% of initial TOC is degraded by ozone/CH compared to 20% by ozone alone with the same total applied ozone of 1.0 mg L^{-1}. Simultaneously, the improvement of removal efficiency of TOC is even more pronounced in the presence of MCH, approximately 63% of initial TOC is removed after 10 min treatment in the process of ozone/MCH.

Furthermore, comparing the removal efficiency of TOC in Fig. 7 with the degradation efficiency of nitrobenzene in Fig. 1 in the same process, it is found that the removal of TOC is lower than the disappearance of nitrobenzene, indicating that nitrobenzene has been mineralized partly into carbon dioxide and water, and the by-products are formed via the degradation of initial compound in the every selected processes.

3.6. The formation and evolution of by-products in the selected processes

Based on the by-products analysis by GC/MS and IC, the experiment identified and compared the formation and evolution

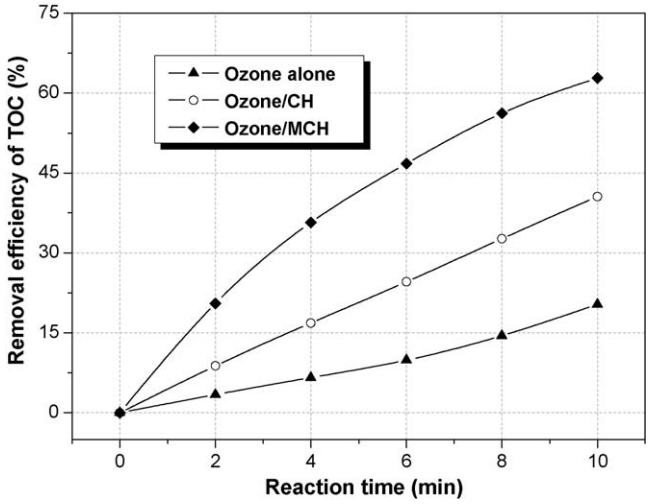

Fig. 7. Comparison of removal efficiency of TOC in the selected processes (reaction conditions as in Fig. 1).

of by-products in the selected processes, and the results are illustrated in Fig. 8.

As can be observed from Fig. 8, in the reaction system of ozone alone, only six by-products are detected: *p*-nitrophenol, *m*-nitrophenol, phenol, malonic acid, 4-nitrocatechol and nitrate ion. On the one hand, *p*-nitrophenol and *m*-nitrophenol can be formed if the attacks of •OH occur respectively at γ- or β-carbons of the benzene ring of nitrobenzene via electrophilic addition [46]. On the other hand, •OH also can attack the nitrobenzene molecule, resulting in the occurrence of electron transfer and denitration, and the formation of phenyl radicals [47]. Phenyl radicals can be transformed into phenol through the further attack of •OH [26]. Furthermore, reactions of the intermediates mentioned above and nitrobenzene with •OH lead to the cleavage of benzene ring and the formation of oxygenated aliphatic compounds, which can be degraded to carboxylic acids via alcohols, aldehydes or ketones (from quinones), for example, malonic acid [26]. The formation of 4-nitrocatechol may be explained by the electrophilic attack of •OH on the *ortho* position of *p*-nitrophenol and *m*-nitrophenol [48], and nitrate ion is a result of the mineralization of organically bound nitrogen during the catalytic ozonation of nitrobenzene. In fact, 4-nitrocatechol can be measured when the concentrations of *p*-nitrophenol and *m*-nitrophenol reach the maximum values.

There are three new by-products to be found in the ozone/CH system: maleic acid, oxalic acid and hydroquinone. The possible contribution of oxidative cleavage of a hydroxylated aromatic compound, derived from the interaction of •OH with nitrophenols, leads to the formation of maleic acid and oxalic acid [49]. The addition of •OH to *p*-nitrophenol results in the formation of hydroquinone, and hydroquinone can also be formed via a simultaneous cleavage of the nitro-group during aromatic nuclear hydroxylation. Otherwise, oxidation of phenol by •OH also can result in hydroquinone formation [50].

It should be noted that 1,2,3-trihydroxy-5-nitrobenzene, acetic acid, *p*-quinone and *o*-nitrophenol, as the novel kinds of by-products compared to those of the process of ozone/CH, appear in the ozone/MCH system. Among these four intermediates, the additional formations of 1,2,3-trihydroxy-5-nitrobenzene and acetic acid are the results of aromatic nuclear hydroxylation of 4-nitrocatechol and the further •OH oxidation of malonic acid, respectively [51,52]. Moreover, *p*-quinone is derived from the further degradation of hydroquinone through the abstraction of two hydrogens [50], and *o*-nitrophenol comes from the •OH attack of nitrobenzene at the α-carbon via electrophilic addition [46].

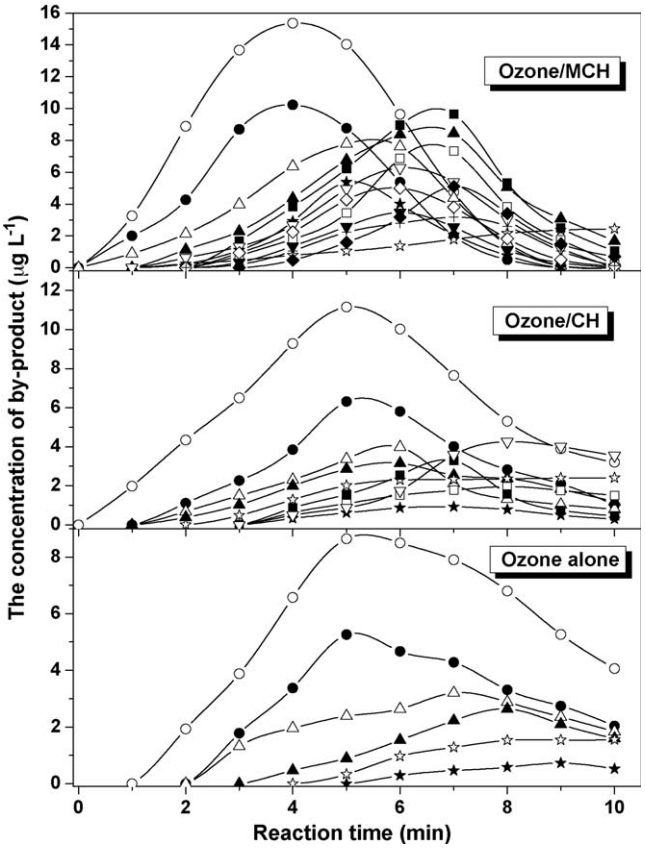

Fig. 8. Formation and evolution of by-products in the selected processes (reaction conditions as in Fig. 1—(○) *p*-nitrophenol; (●) *m*-nitrophenol; (△) phenol; (▲) malonic acid; (☆) nitrate ion; (★) 4-nitrocatechol; (□) maleic acid; (■) oxalic acid; (▽) hydroquinone; (▼) 1,2,3-trihydroxy-5-nitrobenzene; (◇) acetic acid; (◆) *p*-quinone; (+) *o*-nitrophenol).

From Fig. 8 it is also seen that the presence of CH or MCH increases the concentrations and diversities of by-products, and the appearance time of by-products also becomes shorter correspondingly, and the improvement of them is even more pronounced in the presence of MCH. Comparing the results of three processes, it should be remembered that the most by-products achieve nearly the complete conversion in the ozone/MCH system. Though the by-products are rapidly produced from the beginning period of the treatment, they cannot be removed absolutely from aqueous solution to yield other intermediates and/or carbon dioxide and water in the process of ozone/CH. Combined with the results of Figs. 6 and 7, the phenomenon of Fig. 8 suggests that a higher concentration of •OH can lead to the rapid formation of an increasing diversity of by-products, and enhance the total removal of by-products and the degree of mineralization of target organic compound. As far as the two catalytic ozonation processes are concerned, it is revealed that the initiation of •OH is enhanced by the introduction of heterogeneous catalytic surface.

3.7. Discussion on the mechanism

The chemistry of ozone in aqueous solution is complex. Ozone molecular can oxidize water impurities via direct, selective reactions or can undergo decomposition via a chain reaction mechanism resulting in the generation of •OH [53]. The reaction rate constant of nitrobenzene with ozone alone is only $0.09 \pm 0.02\ M^{-1}\ s^{-1}$ [54], while the rate constants for reaction of nitrobenzene with •OH is $2.2 \times 10^8\ M^{-1}\ s^{-1}$ [55]. Therefore, as far as ozonation alone is concerned, the degradation efficiency of nitrobenzene is

Table 1
Comparison of surface characteristics of CH and MCH catalysts.

Catalyst	CH	MCH (1.0% Mn, 0.5% Cu)
BET surface area ($m^2\ g^{-1}$)	0.35	4.38
Total pore volume ($cm^3\ g^{-1}$)	–	0.0066
Average pore diameter (Å)	86.7	55.6
Surface hydroxyl groups ($mol\ m^{-2}$)	0.91×10^{-5}	3.24×10^{-5}
Main phase	$2MgO–2Al_2O_3–5SiO_2$	$2MgO–2Al_2O_3–5SiO_2$, MnO_2, CuO

attributed to the oxidation of •OH generated by the ozone self-decomposition at the conditions of temperature 298 K and initial pH 6.87 in the present experiment from the results described in Fig. 1 [26,27].

Based on the results of Figs. 1, 5 and 6, the reaction in the heterogeneous catalytic ozonation systems should follow apparently the mechanism: chemisorption of ozone on the catalyst surface leading to the formation of active species which react with non-chemisorbed organic molecule. Otherwise, the experiment also determined the characteristics of CH and MCH catalysts, and the results are displayed in Table 1.

As summarized in Table 1, the addition of Mn, Cu and K nitrate salts, as the modifiers, is found to remarkably increase the specific surface area under the experimental conditions to values as high as 4.38 $m^2\ g^{-1}$, i.e., more than 12 times higher than that of the original CH catalyst. The increase in surface area is accompanied by the decrease of average pore diameter from 86.7 to 55.6 Å. On the other hand, the modification of CH catalyst results in the increase in total pore volume. Specifically, the examinations of XRD spectra of CH and MCH samples show that $2MgO–2Al_2O_3–5SiO_2$, the constituent of cordierite, is the main crystal phase of both CH and MCH samples, and the modification of CH catalyst leads to the appearance of additional peaks compared to that obtained with the raw CH, which are MnO_2 and CuO. Results of XRD also identify that the modifier K is found to be X-ray amorphous after the modification of the sample. Furthermore, a good chemical compatibility between the modifiers and the CH is proved because no traces of possible modifier–catalyst reaction products can be detected, namely without any formation of by-products owing to the chemical reaction of CH catalyst itself with the impregnation reagents. Moreover, the determination confirms that there is no effective component leaching during the catalytic ozonation under the present experimental conditions. Combined with the results mentioned above and the characteristics of catalysts listed in Table 1, it can be found that Mn and Cu, as the suitable active components, have the synergistic effect with CH to catalytic ozonation for the degradation of nitrobenzene in aqueous solution. In addition, the results of Table 1 implies that the modification of CH by loading Mn and Cu results in the conversion of surface characteristics, such as the appearance of MnO_2 and CuO crystalline phases, the increase in specific surface area, and the improvement of density of surface hydroxyl groups. Specially, the surface hydroxyl groups on the heterogeneous catalytic surface are believed to be crucial for the initiation of •OH from the decomposition of ozone [29]. The experiments were performed to investigate the effects of modification with Mn and Cu on the density of surface hydroxyl groups. The results are shown in Fig. 9.

As illustrated in Fig. 9(a), the degradation efficiency of nitrobenzene and the density of surface hydroxyl groups all increase with the increase in loading percentages of Mn from 0 to 4.0%. It also can be found that the simultaneous addition of 0.5% Cu with Mn can lead to the remarkable increases in degradation efficiency of nitrobenzene and density of surface hydroxyl groups, meaning that Mn has the synergistic effect with Cu for the improvement of catalytic activity of CH. Furthermore, the results of

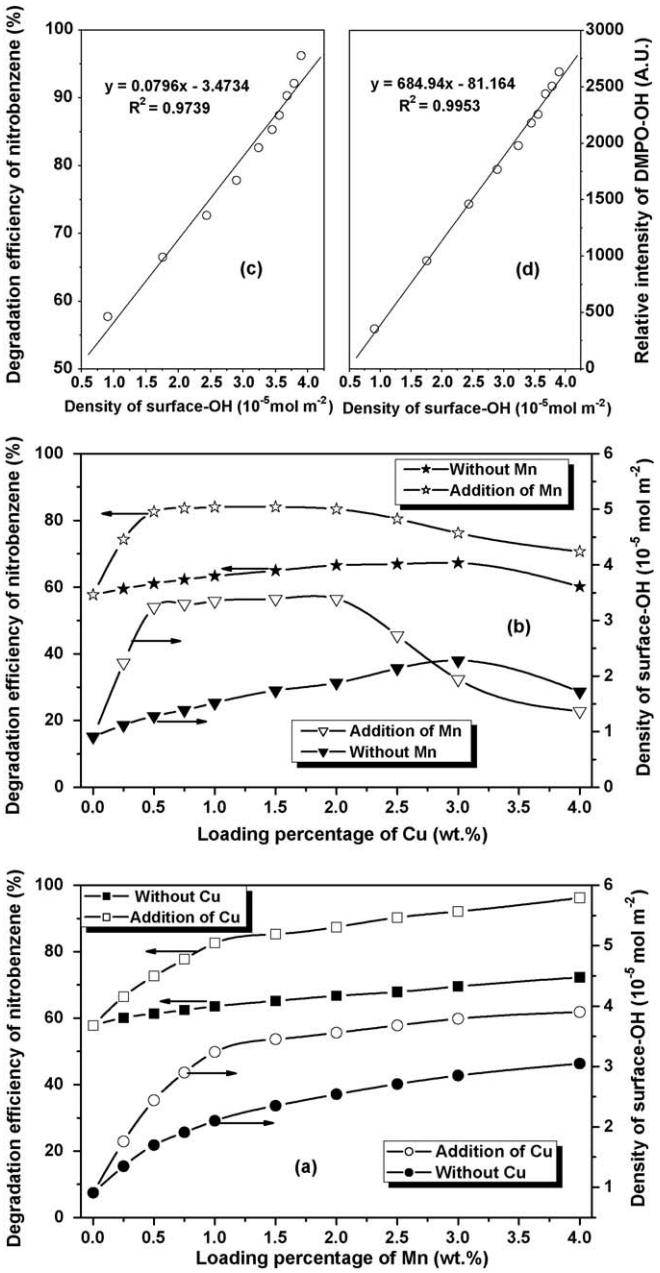

Fig. 9. Effect of loading percentage of metal on the degradation efficiency of nitrobenzene and the density of surface hydroxyl groups (reaction conditions as in Fig. 1; loading percentage of metal (wt.%): 0, 0.25, 0.5, 0.75, 1.0, 1.5, 2.0, 2.5, 3.0 and 4.0%; initial DMPO concentration: 100 mmol L^{-1}; reaction time: 10 min; (a) the conversion of the degradation efficiency of nitrobenzene and the density of surface hydroxyl groups with the loading percentage of Mn; (b) the conversion of the degradation efficiency of nitrobenzene and the density of surface hydroxyl groups with the loading percentage of Cu; (c) the relationship between the degradation efficiency of nitrobenzene and the density of surface hydroxyl groups at the different loading percentage of Mn; (d) the relationship between the density of surface hydroxyl groups and the relative intensity of DMPO–OH adduct signal at the different loading percentage of Mn).

Fig. 9(b) present the complex effects of loading percentages of Cu, indicating that the modification of CH with Cu alone achieves the increases in degradation efficiency and density of surface hydroxyl groups as loading percentage of Cu is increased from 0 to 3.0%, while further increase loading percentage of Cu to 4.0% obtains the negative effect on degradation efficiency and density of surface hydroxyl groups. From Fig. 9(b), it is represented that in the process with addition of 1.0% Mn, the increasing loading per-

centage of Cu from 0 to 0.5% results in the significant enhancements of degradation efficiency and density of surface hydroxyl groups, and then the degradation efficiency of nitrobenzene and the density of surface hydroxyl groups all reach the plateau in the loading percentage range of Cu from 0.5 to 2.0%. Finally, the increasing loading percentage of Cu from 2.0 to 4.0% yields the decreases in degradation efficiency and density of surface hydroxyl groups.

Combining the results of Fig. 9(a) and (b), it is suggested that Mn is the dominating effective component of catalytic activity improvement, and Cu is the subordinate duo to the limited range of loading percentage for the improvement of catalytic activity. Here, metal K cannot be detected in MCH catalyst by XPS and in aqueous solution by ICP, indicating that K may contribute to the structure of space and the distribution of Mn and Cu, and diffuses into aqueous solution after the wet impregnation and the wash by distilled water prior to use, namely K is the assistant effective component for the modification of CH catalyst. Further researches are still needed to find out the function of metal K in the process of modification. In addition, Fig. 9(c) presents the relationship between the degradation efficiency of nitrobenzene and the density of surface hydroxyl groups at the different loading percentages of Mn with the fixed addition of 0.5% Cu, showing a relative good positive correlation. Otherwise, under the same experimental conditions, a relative good correlation is apparent from Fig. 9(d) depicting the relationship between the density of surface hydroxyl groups and the relative intensity of DMPO–OH adduct signal. This phenomenon demonstrates that the degradation efficiency of nitrobenzene is dependent on the density of surface hydroxyl groups, which determines the initiation of $^{\bullet}OH$ from the heterogeneous catalytic surface. Therefore, the possible initiation mechanism of some novel species from the heterogeneous catalytic surface was proposed and illustrated in Fig. 10.

As schematized in Fig. 10, when CH and MCH catalysts made up of metal oxides are introduced into aqueous solution, H_2O molecules will be strongly adsorbed on the metal oxides surface. The adsorbed H_2O always dissociate into $OH^-$and H^+, forming the surface hydroxyl groups with surface cations and oxygen anions, respectively [56]. Then, the chemisorbed surface hydroxyl groups characterize the oxide/water interface. In addition, the surface hydroxyl groups will play an important role in the next step of catalytic ozonation [29].

At first, molecule ozone in aqueous solution can attack the surface hydroxyl group, which was detected on the surface of CH or MCH catalyst, resulting in the occurrence of electron transfer and the release of O_2, and the formation of the surface hydroperoxyl anions (HO_2^-) [41]. Simultaneously, the bond between the heterogeneous surface of catalyst and oxygen atom of the surface HO_2^-(state 3, Fig. 10) is weakened compared to the raw surface hydroxyl group in state 1 due to the interaction of the two oxygen atoms in the surface HO_2^-, one in which comes from molecule ozone. On the one hand, the reaction of the surface $HO_2^-$and another molecule ozone produces one ozonide anion radical ($O_3^{\bullet-}$) and one surface hyperoxyl radical ($HO_2^{\bullet}$). On the other hand, the formation of one $HO_3^{\bullet}$ released to the bulk solution and one surface superoxide anion radical ($O_2^{\bullet-}$) is also possible as a result of the further reaction derived from the surface $HO_2^-$and another molecule ozone. In fact, the surface $HO_2^{\bullet}$ can react further to form the surface $O_2^{\bullet-}$ through the abstraction of one hydrogen ion into aqueous solution, and the formation of the surface $HO_2^{\bullet}$ also can be achieved in the catalytic ozonation by the hydrogen ion addition of the surface $O_2^{\bullet-}$.

The next interactional stage of the heterogeneous surface with molecule ozone implies that the addition of molecule ozone to the surface $O_2^{\bullet-}$ can yield the surface cation (state 6) by the elimination of O_2 and $O_3^{\bullet-}$ to aqueous solution. In addition, the surface cation can adsorb H_2O molecule leading to the formation of the surface hydration cation (H_2O^+, state 7), which will be transformed into the surface hydroxyl group (state 1) with the release of $HO_3^{\bullet}$ in the presence of $O_3^{\bullet-}$ coming from aqueous solution. Thus, the catalyst achieves the regeneration of surface hydroxyl group and the initiation of a radical chain reaction involving the formation of some intermediate species, such as $O_3^{\bullet-}$ and $HO_3^{\bullet}$. Furthermore, the cleavages of the bonds, between the heterogeneous surface and oxygen atom at states 3, 4 and 5 due to the weakening of the bonds, occur to produce the function groups of HO_2^-, $HO_2^{\bullet}$ and $O_2^{\bullet-}$, respectively. Therefore, ozone/CH and ozone/MCH, both composed of heterogeneous and homogeneous catalytic oxidation, will undergo further the multifarious reactions in the homogeneous aqueous solution after the initiation step of radical species from the catalyst surface. The species mentioned above can diffuse rapidly from the catalyst surface or the solid/water interface to aqueous solution, and take part in the next state of radical chain initiation according to the series complex matrix reactions including the initiation, the propagation and the termination, which occur mainly in the homogeneous aqueous phase, in the presence of molecule ozone and H_2O molecule.

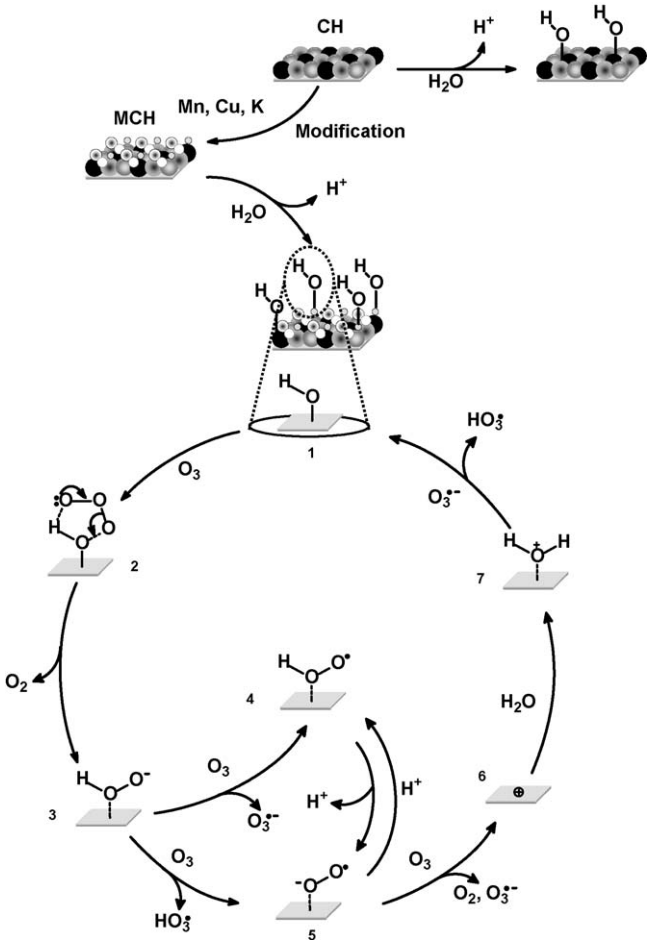

Fig. 10. Scheme of mechanism proposed in the process of catalytic ozonation.

Firstly, the decomposition of ozone generated by the initiator leads to the formation of some intermediate species in homogeneous aqueous solution, such as HO_2^-, $HO_2^{\bullet}$, $O_3^{\bullet-}$, $HO_3^{\bullet}$, $O^{\bullet-}$, $O_2^{\bullet-}$ and $HO_4^{\bullet}$. The CH catalyst can increase the transformation and the decomposition of ozone (Fig. 3(a)) due to the presence of heterogeneous surface, and initiate more quantity of intermediate species in addition to the homogeneous system. The modification of CH with the metals enhances further catalytic effect by the conversion of catalyst characteristics (Fig. 3(b) and Table 1).

Secondly, these species mentioned above may react with each other to form H_2O_2 and •OH, respectively. The formation of H_2O_2 and •OH can be increased in the processes of ozone/CH or ozone/MCH shown in Figs. 5 and 6. More powerful and unselective •OH will degrade nitrobenzene efficiently. This result is in agreement with the phenomenon shown in Fig. 1, which is attributed to the enhanced generation of catalytic surface and the synergistic effect of homogeneous and heterogeneous reactions.

Due to the complex characteristic combined heterogeneous with homogeneous catalytic ozonation, some species generated by the matrix reactions in aqueous solution also can come back to the surface of catalyst through the thin film layer above itself, and subsequently react very fast with some surface functional groups initiated by the interaction of ozone with heterogeneous surface leading to the formation of other species, which will be involved in the next step to accelerate the ozonation process. In conclusion, the synergetic effect mentioned above accelerates the initiation of •OH which determines the degradation efficiency of nitrobenzene.

4. Conclusions

The use of CH or MCH significantly enhances the degradation efficiency of nitrobenzene in aqueous solution by ozonation relative to ozonation alone, owing to the synergistic effect between ozone and the catalysts. The modification process with Mn, Cu and K can remarkably improve the catalytic activity of CH for the ozonation of nitrobenzene. The results suggest that adsorption of nitrobenzene on the surface of CH or MCH is scarcely attributed to the increase in degradation efficiency, and can be neglected compared to the case of ozonation alone and catalytic ozonation. The presence of CH or MCH increases the utilization efficiency of ozone, the concentrations of •OH and H_2O_2 formation, and the removal efficiency of TOC, and the improvement of which is even more pronounced in the presence of MCH. The modification process improves the density of surface hydroxyl groups, which determines the initiation of •OH from the decomposition of ozone on heterogeneous catalytic surface, yielding the acceleration of nitrobenzene degradation in aqueous solution.

Acknowledgements

Authors gratefully acknowledge the Scheme of 863 High Technology Research and Development Program of China (Grant No. 2006AA06Z306), the National Natural Science Foundation of China (Grant No. 50578051) and the China Postdoctoral Science Foundation (Grant No. 20080440130) for the financial support of this study.

References

[1] W.D. Bellamy, F. Damez, B. Langlais, A. Montiel, K.L. Rakness, D.A. Reckhow, C.M. Robson, in: B. Langlais, D.A. Reckhow, D.R. Brink (Eds.), Ozone in Water Treatment: Application and Engineering, Lewis Publishers, Chelsea, MI, USA, 1991, pp. 317–468.
[2] B. Legube, V.L.N. Karpel, Catal. Today 53 (1999) 61–72.
[3] B.S. Kim, H. Fujita, Y. Sakai, A. Sakoda, M. Suzuki, Water Sci. Technol. 46 (2002) 35–41.
[4] R. Mantha, K.E. Taylor, N. Biswas, J.K. Bewter, Environ. Sci. Technol. 35 (2001) 3231–3236.
[5] Y. Mu, H.Q. Yu, J.C. Zheng, S.J. Zhang, G.-P. Sheng, Chemosphere 54 (2004) 789–794.
[6] J.S. Zhao, O.P. Ward, P. Lubicki, J.D. Cross, P. Huck, Biotechnol. Bioeng. 73 (2001) 306–312.
[7] S. Contreras, M. Rodríguez, E. Chamarro, S. Esplugas, J. Photochem. Photobiol. A 142 (2001) 79–83.
[8] J. Sarasa, M.P. Roche, M.P. Ormad, E. Gimeno, A. Puig, J.L. Ovelleiro, Water Res. 32 (1998) 2721–2727.
[9] L.S. Bell, J.F. Devlin, R.W. Gillham, P.J. Binning, J. Contam. Hydrol. 66 (2003) 201–217.
[10] M. Rodriguez, V. Timokhin, F. Michl, S. Contreras, J. Gimenez, S. Esplugas, Catal. Today 76 (2002) 291–300.
[11] C.L. Zheng, J.T. Zhou, J. Wang, J. Wang, B.C. Qu, J. Hazard. Mater. 160 (2008) 194–199.
[12] H.X. Ai, J.T. Zhou, H. Lv, J. Wang, J.B. Guo, G.F. Liu, Y.Y. Qu, J. Environ. Sci. 20 (2008) 865–870.
[13] J.F. Wu, C.Y. Jiang, B.J. Wang, Y.F. Ma, Z.P. Liu, S.J. Liu, Appl. Environ. Microbiol. 72 (2006) 1759–1765.
[14] Z.L. Li, M. Yang, D. Li, R. Qi, H.J. Liu, J.F. Sun, J.H. Qu, J. Environ. Sci. 20 (2008) 778–786.
[15] R.P. Liu, H.J. Liu, D.J. Wan, J.H. Qu, M. Yang, J. Environ. Sci. 21 (2008) 796–802.
[16] A.M. Wang, C. Hu, J.H. Qu, M. Yang, H.J. Liu, J. Ru, J. Environ. Sci. 20 (2008) 787–795.
[17] R.J. Tayade, R.G. Kulkarni, R.V. Jasra, Ind. Eng. Chem. Res. 45 (2006) 922–927.
[18] Y. Arai, K. Tanaka, A.L. Khlaifat, J. Mol. Catal. A: Chem. 243 (2006) 85–88.
[19] M.H. Priya, G. Madras, J. Photochem. Photobiol. A 178 (2006) 1–7.
[20] R.M. Mohamed, J. Mater. Process. Technol. 209 (2009) 577–583.
[21] D. Cropek, P.A. Kemme, O.V. Makarova, L.X. Chen, T. Rajh, J. Phys. Chem. C 112 (2008) 8311–8318.
[22] M. Rodriguez, A. Kirchner, S. Contreras, E. Chamarro, S. Esplugas, J. Photochem. Photobiol. A 133 (2000) 123–127.
[23] I. Arslan-Alaton, J.L. Ferry, Appl. Catal. B: Environ. 38 (2002) 283–293.
[24] Y.X. Yang, J. Ma, Q.D. Qin, X.D. Zhai, J. Mol. Catal. A: Chem. 267 (2007) 41–48.
[25] J. Ma, M.H. Sui, T. Zhang, C.Y. Guan, Water Res. 39 (2005) 779–786.
[26] L. Zhao, J. Ma, Z.Z. Sun, Appl. Catal. B: Environ. 79 (2008) 244–253.
[27] L. Zhao, J. Ma, Z.Z. Sun, X.D. Zhai, Appl. Catal. B: Environ. 83 (2008) 256–264.
[28] T. Zhang, J. Ma, J. Mol. Catal. A: Chem. 279 (2007) 82–89.
[29] J. Ma, N.J.D. Graham, Water Res. 33 (1999) 785–793.
[30] J. Ma, N.J.D. Graham, Water Res. 34 (2000) 3822–3828.
[31] J.H. Qu, H.Y. Li, H.J. Liu, H. He, Catal. Today 90 (2004) 291–296.
[32] K.L. Rakness, G. Gordon, B. Langlais, W. Masschelein, N. Matsumoto, Y. Richard, C.M. Robson, I. Somiya, Ozone Sci. Eng. 18 (1996) 209–229.
[33] H. Bader, J. Hoigné, Water Res. 15 (1981) 449–456.
[34] H. Bader, V. Sturzenegger, J. Hoigné, Water Res. 22 (1988) 1109–1115.
[35] E. Laiti, L.O. Öhman, J. Nordin, S. Sjöberg, J. Colloid Interface Sci. 175 (1995) 230–238.
[36] H. Tamura, A. Tanaka, K.Y. Mita, R. Furuichi, J. Colloid Interface Sci. 209 (1999) 225–231.
[37] J.S. Noh, J.A. Schwarz, J. Colloid Interface Sci. 130 (1989) 157–164.
[38] J.S. Noh, J.A. Schwarz, Carbon 28 (1990) 675–682.
[39] C. Cooper, R. Burch, Water Res. 33 (1999) 3695–3700.
[40] F.J. Beltrán, J. Rivas, P.M. Álvarez, M.A. Alonso, B. Acedo, Ind. Eng. Chem. Res. 38 (1999) 4189–4199.
[41] M. Ernst, F. Lurot, J.C. Schrotter, Appl. Catal. B: Environ. 47 (2004) 15–25.
[42] J. Staehelin, R.E. Buhler, J. Hoigné, J. Phys. Chem. 88 (1984) 5999–6004.
[43] E.G. Janzen, B.J. Blackburn, J. Am. Chem. Soc. 91 (1969) 4481–4490.
[44] H. Utsumi, M. Hakoda, S. Shimbara, H. Nagaoka, Y. Chung, A. Hamada, Water Sci. Technol. 30 (1994) 91–99.
[45] S.K. Han, S.N. Nam, J.W. Kang, Water Sci. Technol. 46 (2002) 7–12.
[46] D.S. Bhatkhande, V.G. Pangarkar, A.A.C.M. Beenackers, Water Res. 37 (2003) 1223–1230.
[47] Q.-R. Li, C.-Z. Gu, Y. Di, H. Yin, J.-Y. Zhang, J. Hazard. Mater. B 133 (2006) 68–74.
[48] A. Di Paola, V. Augugliaro, L. Palmisano, G. Pantaleo, E. Savinov, J. Photochem. Photobiol. A 155 (2003) 207–214.
[49] A. Goi, M. Trapido, T. Tuhkanen, Adv. Environ. Res. 8 (2004) 303–311.
[50] E. Brillas, E. Mur, R. Sauleda, L. Sànchez, J. Peral, X. Domènech, J. Casado, Appl. Catal. B: Environ. 16 (1998) 31–42.
[51] M.A. Oturan, J. Peiroten, P. Chartrin, A.J. Acher, Environ. Sci. Technol. 34 (2000) 3474–3479.
[52] J. Kiwi, C. Pulgarin, P. Peringer, Appl. Catal. B: Environ. 3 (1994) 335–350.
[53] B. Kasprzyk-Hordern, M. Ziółek, J. Nawrocki, Appl. Catal. B: Environ. 46 (2003) 639–669.
[54] J. Hoigné, H. Bader, Water Res. 17 (1983) 173–183.
[55] J. Hoigné, H. Bader, Water Res. 10 (1976) 377–386.
[56] Y. Joseph, W. Ranke, W. Weiss, J. Phys. Chem. B 104 (2000) 3224–3236.